Journal of Nanotechnology

WILEY

RESEARCH ARTICLE OPEN ACCESS

Development of Niosome-Encapsulated Standardized Water Extract of *Eurycoma longifolia* for Potential Immunomodulatory Activity In Vitro

Muhammad Nor Farhan Saat[1,2] | Norazlinaliza Salim[2,3] | Wan Abdul Hakim Wan Lokman[1] | Nabilah Md Razak[1] | Mohd Basyaruddin Abdul Rahman[2] | Murizal Zainol[1] | Azren Aida Asmawi[2,4] | Mohd Ridzuan Mohd Abd Razak[1]

[1]Herbal Medicine Research Centre, Institute for Medical Research, National Institutes of Health, Ministry of Health, Malaysia, Setia Alam, Shah Alam, Selangor 40170, Malaysia | [2]Department of Chemistry, Faculty of Science, Universiti Putra Malaysia, Serdang, Selangor 43400 UPM, Malaysia | [3]Centre for Foundation Studies in Science, Universiti Putra Malaysia, Serdang, Selangor 43400 UPM, Malaysia | [4]Department of Pharmaceutical Technology, Faculty of Pharmacy and Biomedical Sciences, MAHSA University, Bandar Saujana Putra, Jenjarom, Selangor 42610, Malaysia

Correspondence: Muhammad Nor Farhan Saat (mnfarhan@moh.gov.my) | Norazlinaliza Salim (azlinalizas@upm.edu.my)

Received: 14 August 2025 | **Revised:** 24 April 2026 | **Accepted:** 29 April 2026

Academic Editor: Sudipta Panja

Keywords: *Eurycoma longifolia* | immunomodulatory activity | nanoformulation | niosome

ABSTRACT

Eurycoma longifolia is a well-known medicinal plant recognized for its anticancer activity and immunomodulatory properties. Despite its therapeutic potential, the extract has demonstrated low bioavailability, particularly due to the limited permeability of eurycomanone in rodent studies. The objectives of the present study were to develop a niosome formulation incorporating a standardized water extract of *E. longifolia* and to evaluate its immunomodulatory activity. Three niosome formulations containing *E. longifolia* extract with different stabilizers were prepared using the heating method and were abbreviated based on the stabilizing agent used: Nio1, containing sodium dodecyl sulfate (SDS); Nio2, containing α-tocopherol; and Nio3, containing phenonip. The prepared niosomes were characterized for their physicochemical properties, including particle size, polydispersity index (PDI), zeta potential, pH, stability, entrapment efficiency (EE), and in vitro drug release. All niosome formulations exhibited desirable particle size (195–493 nm), low PDI values (0.05–0.13), and negative zeta potentials (−30.63 to −44.90 mV) with pH values ranging from 7.05 to 7.55. The formulations remained physically stable at room temperature over the 3-month storage period. EE ranged from 59.50% to 66.90%. In vitro drug release at pH 1.2, 6.8, and 7.4 demonstrated a diffusion-controlled release mechanism. An in vitro cell viability and an immunomodulatory assay of the niosome on the lipopolysaccharides (LPS)-induced murine macrophage (RAW264.7) cell line was evaluated. Cytotoxicity data showed that the Nio2 formulation was less toxic towards the Vero, THP-1, and RAW 264.7 cells with IC_{50} values of 19.90, 22.78, and 23.87 μg/mL, respectively. Immunomodulatory assays demonstrated that Nio2 treatment significantly suppressed nitric oxide release in LPS-stimulated murine macrophages. The Nio2 formulation also enhanced the phagocytic ability of THP-1 cells towards *E. coli*, similar to the nonformulated *E. longifolia* extract. These results indicate that Nio2 could serve as effective nanocarriers for enhancing immunomodulatory activity by activating the THP-1 cells and potentially benefiting macrophage cells. In conclusion, this study demonstrates that the niosome formulation incorporating a standardized water extract of *E. longifolia* was successfully developed and exhibits potential immunomodulatory activity, supporting its further evaluation in in vivo immunomodulatory study.

1 | Introduction

Viral infectious diseases remain a persistent global health threat due to the continuous emergence of new pathogens [1]. These viruses are responsible for widespread illnesses such as influenza, HIV, measles, Zika, Chikungunya, and COVID-19, with dengue infection continuing to rise in both incidence and severity [1]. According to the World Health Organization, more than five million dengue cases and 5000 deaths were reported across over 80 countries [2]. In Malaysia, dengue has become a major public health concern, with a 1561% increase in reported cases from 1995 to 2014 [3]. Dengue can be asymptomatic or cause mild fever; however, in severe cases, it progresses to haemorrhagic dengue fever, which involves vascular leakage, bleeding, and organ dysfunction. These complications are largely attributed to dysregulated host immune, known as a cytokine storm, where the body releases excessive amounts of pro-inflammatory and regulatory cytokines like IL-6, IL-8, IL-10, IL-15, TNF-α, MCP-1, and IFN-γ [4]. If uncontrolled, this immune overactivation can result in systemic inflammation and multiorgan failure. Hence, modulation of excessive cytokine production represents a critical therapeutic target for mitigating severe dengue-associated immunopathology. Therefore, immunomodulatory therapies have recently gained attention as complementary strategies for managing viral infections, including dengue [5].

Eurycoma longifolia, commonly known as Tongkat Ali, is a flowering medicinal shrub native to Southeast Asia and widely recognized in traditional medicine [6]. It has been used to treat intermittent fever, diarrhea, and fatigue, with its roots applied for a range of ailments including cough, dysentery, hypertension, and bleeding [7, 8]. Pharmacological studies confirm that *E. longifolia* possesses anti-inflammatory, antimalarial, antiulcer, and anticancer properties [6]. These bioactivities are linked to the plant's rich content of phenolics, quassinoids, alkaloids (canthin-6-one, β-carbolines), triterpenes, neolignans, lactones, and steroids [9, 10]. Among these, eurycomanone is the common compound and is widely used as a chemical marker for extract standardization [11]. The immune system can be regulated by both internal and external stimuli, and immunomodulators—whether synthetic or natural—help to enhance or suppress immune functions [12]. Natural products often stimulate innate immune responses by activating macrophages, monocytes, neutrophils, and cytokines [13]. Herbal remedies have long been used to reduce inflammation, with quassinoids from *E. longifolia* shown to contribute to its anti-inflammatory potential [14, 15]. In a study by Hien et al., an alkaloid-rich fraction (ELA) inhibited lipopolysaccharides (LPS)-induced nitric oxide (NO) and protein expression in vitro and in mice, demonstrating strong anti-inflammatory effects [16]. Other isolated compounds also suppressed the expression of IL-6, iNOS, and NF-κB in response to LPS, indicating action via the NF-κB pathway [17].

Despite its promising biological activities, the standardized water extract of *E. longifolia* has shown low bioavailability in rodents, which may limit its therapeutic impact as an immunomodulator [11, 18]. To overcome this challenge, nanocarrier-based systems such as niosomes have been proposed to improve both delivery and bioavailability. Niosomes are vesicular carriers formed by nonionic surfactants and cholesterol, offering advantages like enhanced solubility, stability, biocompatibility, and controlled release of active compounds [19]. Recent studies have demonstrated that niosomal delivery of plant extracts such as *Garcinia mangostana*, *Zingiber officinale*, and *Knema retusa* enhances biological activity while reducing cytotoxicity and improving targeted effects [20–23]. They are known to improve pharmacokinetics and pharmacodynamics while also reducing systemic toxicity by enabling site-specific targeting [20–24]. These properties make them suitable for delivering plant-derived compounds with poor water solubility. Surfactants, essential to niosome structure, significantly influence membrane fluidity, permeability, and drug retention, which in turn affect the efficiency and safety of the formulation [25, 26].

Research on niosomes encapsulating *E. longifolia* for immunomodulatory purposes is currently lacking. Therefore, this study aims to prepare a niosomal formulation containing standardized *E. longifolia* root water extract. The formulation undergoes physicochemical characterization and stability evaluation. The in vitro drug release and its potential immunomodulatory activity were also evaluated.

2 | Methodology

2.1 | Chemicals and Materials

Standardized water extract of *E. longifolia* (root) was purchased from Biotropic, Malaysia. The term "standardized" refers to the consistent percentage of eurycomanone maintained in every batch of *E. longifolia* root water extract produced by Biotropics. According to the certificate of analysis provided upon purchase, the eurycomanone content is standardized within the range of 0.8%–1.5%. Polyoxyethylene sorbitan tristearate (Tween 60) and sorbitan monostearate (Span 60) were purchased from Sigma-Aldrich (St. Louis, USA). Phenonip, sodium chloride (NaCl), cholesterol, α-tocopherol, curcumin, and PBS (pH 7.4) were purchased from Merck (Germany). Glycerol, Dulbecco's modified Eagle's medium (DMEM) culture medium, fetal bovine serum (FBS), penicillin-streptomycin (PS), 4′,6-diamidino-2-phenylindole (DAPI), LPS, Griess reagent kit, and sodium nitrate ($NaNO_3$) were purchased from Fisher Scientific (Loughborough, USA). CellTiter-Glo cell viability assay was purchased from Promega (Madison, USA). A phagocytosis assay kit (IgG-FITC) was purchased from Cayman Chemical (Michigan, USA). African Green Monkey kidney (Vero), human monocyte (THP-1), and murine macrophage (RAW 264.7) cell lines were purchased from the American Type Culture Collection (ATCC, Virginia, USA).

2.2 | Characteristic of Eurycomanone From *E. longifolia* and Preparation of *E. longifolia* Extract-Loaded Niosome Formulations

The characteristics of eurycomanone, a major bioactive compound in *E. longifolia*, were obtained from previously published data [11]. Based on data, niosomes were prepared using the heating method described by Mohamad Saimi et al. [27] with some modifications. Based on their particle size and physical stability following centrifugation test, three formulations with different stabilizers (as shown in Table 1) were selected for this study, as determined from a preliminary investigation (Table S1, Supporting Information). Initially, for the lipid phase, a combination of surfactants (Tween 60:Span 60 with a ratio of 2:1) was

TABLE 1 | The composition of the niosome formulations.

Niosome formulation	Composition (% w/w)		
	Nio1	Nio2	Nio3
Tween 60: Span 60 (2:1)	2.00	2.00	2.00
Cholesterol	1.01	1.01	1.01
3% Glycerol in phosphate buffer saline	63.06	63.06	63.06
Sodium dodecyl sulfate (SDS)	0.50	—	—
α-Tocopherol	—	0.50	—
Phenonip	—	—	0.50
Standardized water extract of *E. longifolia*	0.10	0.10	0.10
Deionized water	33.33	33.33	33.33

mixed using a magnetic stirrer at 800 rpm, 120°C for 5 min in a glass Schott bottle. Cholesterol was added to the mixture and then continuously mixed and heated at 120°C for 30 min SDS was added to the mixture, which was continuously mixed and heated at 120°C, 800 rpm for 30 min. Glycerol solution 3% w/w in PBS pH 7.4 was added into the mixture dropwise while continuously heated at 60°C for 45 min.

For the remaining formulations, SDS was replaced with either α-tocopherol or Phenonip, while all other formulation components and preparation conditions were kept identical.

For the aqueous phase, standardized water extract of *E. longifolia* 0.1% (w/w) root water extract was mixed in deionized water using a magnetic stirrer at 800 rpm for 15 min. Then, the mixture was added into the lipid phase and continuously homogenized by a magnetic stirrer at 1000 rpm, 60°C, for 60 min. Finally, the mixture was sonicated using a probe sonicator (Qsonica, Newtown, CT, USA) for 30-s "on" and 5-s "off" for five cycles, amplitude of 75%.

2.3 | Physicochemical Characterization

2.3.1 | Particle Size, Polydispersity Index (PDI) and Zeta Potential Measurement

The dynamic light scattering (DLS) technique was utilized to evaluate the particle size and PDI. The approach involved scattering light at a temperature of 25°C and an angle of 173°. The device used for this procedure was the Malvern Nano ZS90 (Malvern, USA). The niosome formulation was diluted with PBS (1:100) and then added to the sample cell. Three measurements were performed in triplicate. The particle size of the niosome formulations was maintained below 500 nm, as this range is considered desirable for oral administration due to its association with improved gastrointestinal (GI) absorption, enhanced epithelial penetration, and increased oral bioavailability [28]. The calculation of zeta potential was performed based on the measurement of the electrophoretic mobility of dispersed particles in a charged field.

2.3.2 | Morphology of the Formulation

Transmission electron microscopy (TEM) was used to examine the shape of niosome by dropping a droplet of niosome solution onto copper grids coated with carbon (400-mesh holes). Niosome formulation at pH 7.4 diluted 1:100 with PBS. Subsequently, 1% uranyl acetate was used to negatively stain the sample for 10 min at room temperature. The noisy sample-containing grid was inspected using a Hitachi H-7100 transmission electron microscope (Tokyo, Japan) after the excess liquid was filtered out with filter paper.

2.3.3 | pH Measurement

The pH of the niosome formulations was measured at room temperature using a pH meter (Mettler-Toledo, Switzerland). The pH meter was calibrated using pH standard buffer solutions before taking measurements. After taking three measurements data, the average was calculated.

2.3.4 | Stability Study

Freshly prepared niosome formulations were transferred to six centrifuge tubes and centrifuged at 4000 rpm for 15 min at room temperature (27°C) using a bench-top centrifuge. This test was performed to assess the short-term physical stability of the formulations by accelerating potential instability phenomena such as phase separation, vesicle aggregation, or precipitation. After centrifugation, samples were visually inspected for any signs of creaming, sedimentation, or phase separation. Subsequently, the formulations were stored at 27°C for up to 90 days, during which particle size, PDI, and physical appearance (color change or phase separation) were periodically evaluated to monitor long-term physical stability.

2.4 | Drug Entrapment Efficiency (EE) Measurement

EE % can be determined using centrifugation of 1 mL of the formulation at 21,000 rpm for 1 h. Following centrifugation, the niosome formulation was collected as a pellet, while the unencapsulated *E. longifolia* extract remained in the supernatant. The supernatant and the sediment were separated and then diluted to 25 mL with PBS pH 7.4, filtered using a PTFE syringe filter (0.22 μm pore size, Membrane Solutions, Auburn, WA, USA), and then measured using a UV–vis spectrophotometer (Beckman, DU 530, Fullerton, CA, USA) at λ_{max} 250 nm for eurycomanone. Using the following equation, the percentage of drug entrapment in niosomes was calculated.

$$\text{Entrapment efficiency } \% = \left(\frac{(\text{Total drug} - \text{drug in the supernatant})}{\text{Total drug}}\right) \times 100\%. \quad (1)$$

2.5 | In Vitro Drug Release Study

The diffusion of formulations was studied using the dialysis bag diffusion technique. Cellulose membranes were soaked in the release medium. Then, niosome formulations were placed into the dialysis bag. Both ends of the bag were tied and then carefully immersed in a beaker containing PBS at pH 7.4, which mimicked the ileum's pH condition. The elution medium was stirred using a magnetic bar at 100 rpm. One milliliter of the receptor medium was withdrawn at different time intervals (typically at 1, 2, 3, 4, 5, 6, 7, 8, 12, and 24 h) and then replaced with the same volume of fresh media to maintain the sink conditions. These procedures were repeated with PBS pH 6.8, which mimicked the duodenum pH, and hydrochloric acid (HCl) pH 1.2 mimicked the stomach. All experiments were carried out in triplicate. The selected pH conditions were employed to reflect physiological pH variations along different regions of the GI tract and to evaluate the stability and release behavior of the niosome-encapsulated formulation during GI transit. These samples were analyzed using a UV–vis spectrophotometer (Beckman, DU 530, Switzerland) at λ_{max} 250 nm for eurycomanone. The calibration curves for eurycomanone were used to determine the cumulative percentage of eurycomanone released. The amount of drug released from NGC was calculated using the following equation:

$$\text{drug release } \% = \left(\frac{(M_d \times \text{V})}{\text{M°d}}\right) \times 100\%, \tag{2}$$

where M_d is the concentration of eurycomanone released in the receptor medium collected, measured using a UV–vis spectrophotometer at λ_{max} 250 nm, V is the volume of the release media, and M°d is the total amount of eurycomanone loaded in the formulation.

2.5.1 | Kinetic Release Study

The following mathematical models were used to evaluate the kinetics and mechanism of drug release from optimized niosome formulation: zero-order (cumulative amount of drug release versus time, Equation (3)), first-order (log the cumulative amount of drug remaining versus time, Equation (4)), Higuchi (cumulative percentage of drug release versus square root of time, Equation (5)), Hixson–Crowell (cube root cumulative amount of drug remaining versus time, Equation (6)), and Korsmeyer–Peppas (log cumulative percentage of drug release versus log time, Equation (7)). The model that best fit the drug release data was selected based on the correlation coefficient (R^2) value obtained from the plotted graph in various models. The model that gave the highest value was considered as the best fit for release data.

$$M_t = M_0 + k_0 t, \tag{3}$$

$$\ln M_0 - M_t = \ln M_0 + k_1 t, \tag{4}$$

$$M_t = k_H t^{1/2}, \tag{5}$$

$$M_0{}^{1/3} - M_t{}^{1/3} = k_{\text{HC}} t, \tag{6}$$

$$\frac{M_t}{M_\infty} = k_{\text{KP}} t^n, \tag{7}$$

where M_0 is the initial amount of drug in dissolution media; M_t is the amount of drug released in time t; k_0, k_1, k_H, k_{HC}, and k_{KP} are the release rate constants; M_t/M_∞ is the fraction of drug release over time; n is the release exponent indicating the mechanism; and t is time.

2.6 | In Vitro Cytotoxicity Study

The cytotoxicity of the niosome formulations and *E. longifolia* standardized water extract was assessed using the ATP luciferase assay following exposure to the African Green Monkey kidney (Vero), human monocyte (THP-1), and murine macrophage (RAW 264.7) cell lines. On 96-well microplates, 100 μL of a concentration of 5×10^3 cells per mL was produced and seeded. Following a 72-h incubation period, the samples were diluted and added to each well at the specified concentrations of 62.50, 31.25, 15.62, 7.81, 3.60, 1.95, and 0.97 μg/mL. Each well received an addition of ATP luciferase reagent, which was then incubated for 10 min at room temperature. The SPECTROstar Omega microplate reader (Ortenberg, Germany) was used to measure the luminescent signal. Using the following equation, cytotoxicity was defined as the drug concentration that resulted in a 50% growth inhibition of the cells (IC_{50} value):

$$\text{cell viability} = \frac{\text{luminescence of sample}}{\text{luminescence of control}} \times 100\%. \tag{8}$$

After the determination of the percentage of cell viability was completed, graphs of the percentage of cell viability against their respective concentration were plotted. Three replicates of the measurement were made.

2.7 | NO Release Assay

The inhibitory effects of test compounds on NO production, which reflect the anti-inflammatory activity, were evaluated in LPS-activated RAW 264.7 cells. The cells were seeded in a 96-well plate at a density of 1×10^6 cells per well and incubated at 37°C for 24 h in a humidified atmosphere containing 5% CO_2. The cells were treated with 1 μg/mL of LPS for 24 h and continued to be treated with the sample tested (Nio2 and *E. longifolia* extract) at a concentration of 12.5 μg/mL. LPS control and curcumin-treated stimulated cells were used as negative and positive controls, respectively. Nitrite levels in the cultured media were determined by the Griess Reagent kit (G7921; Fisher Scientific). Briefly, cells were dispensed into 96-well plates and 100 μL of each supernatant was mixed with the same volume of Griess reagent (1% sulphanilamide, 0.1% N-(1-naphthyl)ethylenediamine dihydrochloride, and 5% phosphoric acid) and incubated at room temperature for 10 min. The NO production in the assay was determined by measuring the absorbance of the purple azo formed after the addition of the Griess reagent to each well. A standard curve of known concentrations of sodium nitrite ($NaNO_2$) was plotted and absorbance readings were measured at 550 nm using the SPECTRO star Omega microplate reader (Ortenberg, Germany). Sodium nitrite was used as a standard to measure the concentration of nitrite present in each well of the microplate, which was defined as an indirect measurement of NO production. The percentage of NO inhibition was calculated relative to the LPS-induced control group, which was defined as exhibiting 0% NO inhibition.

2.8 | Phagocytic Ability Assay

The phagocytic ability of THP-1 cells was evaluated using a phagocytosis assay kit (IgG-FITC, Item No. 500290; Cayman Chemicals). The protocol of the assay followed the manufacturer's instructions. The cells were seeded in a 96-well microplate at a density of 5×10^3 cells per well and cultured overnight at 37°C to allow adherence to the plate. After treatment with 1 μg/mL of LPS from *Escherichia coli*, the cells were exposed to the sample tested (Nio2, *E. longifolia* extract) at a concentration of 12.5 μg/mL. Untreated and curcumin-treated stimulated cells were used as negative and positive controls, respectively. Latex Beads-Rabbit IgG-FITC Complex was added directly to the culture medium at a dilution of 1:200 and incubated at 37°C for 1 h. The cells were washed twice using the supplied assay buffer. The DAPI stain was added to each well and washed again using a supplied buffer and further visualized using the Operetta High Content Analysis system (PerkinElmer, USA). Phagocytic activity was determined as the percentage of engulfed fluorescent beads by the cell.

$$\text{phagocytic ability} = \frac{\text{number of engulfed fluorescent beads in a cell}}{\text{total number of cells}} \times 100\%. \quad (9)$$

2.9 | Statistical Analysis

All experiments were carried out in triplicate, and data are expressed as mean ± standard deviation (SD). Statistical analysis was performed using one-way analysis of variance (ANOVA), followed by Tukey's post hoc test to determine significant differences between the niosome formulations. A p-value of less than 0.05 was considered statistically significant.

3 | Results and Discussion

3.1 | Characterization of Erycomanone and *E. longifolia* Extract–Loaded Niosome Formulation

The rationale for encapsulating the *E. longifolia* extract in a niosome system is supported by the physicochemical properties of its major active compound, eurycomanone. According to the previously published data [11], eurycomanone exhibits high aqueous solubility at both pH 5.4 and 7.4 and a low distribution coefficient, log D value (−0.35), indicating a hydrophilic profile. Additionally, it is also reported to be chemically stable across different pH conditions that mimic physiological environments, including pH 2.0 (gastric), 5.0 (fed-state intestinal), and 6.5 (fasted-state intestinal). These characteristics suggest that eurycomanone is well suited for encapsulation in niosomes, which can protect hydrophilic and sensitive compounds while improving their delivery and bioavailability. Based on these considerations, a niosome system was selected as the vesicular platform for this study. Niosomes, which are composed of nonionic surfactants, have been widely reported to efficiently encapsulate hydrophilic compounds within their aqueous core while providing good membrane stability and formulation robustness [19]. Accordingly, the formulations were optimized through the incorporation of stabilizing agents with complementary functional roles to preserve vesicle integrity and enhance encapsulation efficiency and stability.

In order to increase the therapeutic activity of standardized *E. longifolia* extract due to its poor bioavailability, three niosome formulations were synthesized according to Table 1. The stability of the niosome formulation can be affected by the type of surfactant used [29]. Cholesterol is one of the important lipid components used in niosome formulation, with the function of stabilizing the niosome membrane and influencing the physical properties and structure of the niosome [30]. The selection of SDS, α-tocopherol, and Phenonip was based on their distinct stabilizing mechanisms, and each was evaluated in different niosomal formulations to investigate their individual contributions to niosome stability. SDS was selected as a surfactant because it increases the surface charge of the niosomes, thereby enhancing electrostatic repulsion between vesicles and improving the stability of the niosome membrane structure [31]. α-Tocopherol was incorporated to increase encapsulation efficiency while providing antioxidant protection to the niosome system, helping to preserve both the membrane components and the encapsulated extract from oxidative degradation [25]. Phenonip was included as a preservative to maintain formulation stability during storage by reducing stability impairment of the niosome membrane structure associated with microbial contamination [32]. Overall, the use of different stabilizing agents in separate formulations enabled a systematic evaluation of their effects on the physicochemical stability and performance of the niosomal delivery system.

3.2 | Physicochemical Characterization

3.2.1 | Particle Size, PDI, and Zeta Potential

All three niosome formulation mixtures with uniform creamy dispersion appearance with no separation layer were observed (Figure 1(a)). The particle sizes of Nio1, Nio2, and Nio3 were 195.57 ± 4.35 nm, 221.03 ± 0.986 nm, and 493.16 ± 8.60 nm, respectively, with Nio1 having the smallest particle size. The particle size formed was influenced by the concentration and nature of surfactant, stabilizer, bioactive component, and preparation method [25]. SDS in the Nio1 formulation plays the role as a charge inducer, which can reduce molecular aggregates formed by surfactant. It has been reported that the addition of SDS to the formulation can reduce the particle size of the niosome [31]. The uniformity of particle size in the niosome mixtures is indicated by PDI values of 0.11, 0.05, and 0.13 for Nio1, Nio2, and Nio3, respectively, as shown in Table 2. These PDI results indicate that all three formulations are considered to be monodispersed and stable nanocarriers. Measurement of the PDI value can determine the degree of polydispersity based on the width of the sample size distribution in the niosome system [32]. When the PDI value is less than 0.4, it represents a low level of aggregation profile and a monodisperse system of niosome [33].

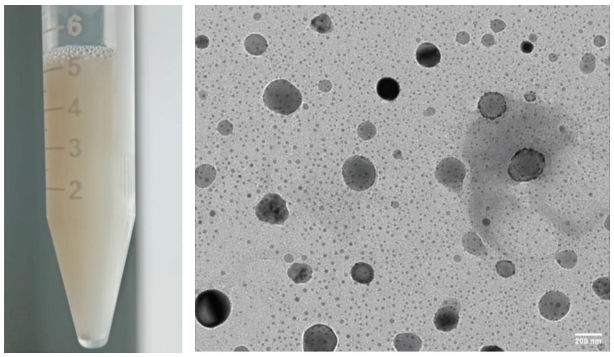

(a) (b)

FIGURE 1 | (a) Representative of a niosome formulation containing the standardized water extract of *E. longifolia* (Nio2), and its (b) TEM image.

The zeta potential values for the three niosome formulations indicate that all samples possess a negatively charged surface, which is stable against aggregation and fusion due to the enhanced electrostatic repulsion between particles [27]. Among the three formulations, Nio2 exhibited the most negative zeta potential value. At pH 7.4, α-tocopherol, which has a high pKa (12–13), remains largely un-ionized and is therefore unlikely to contribute directly to the negative surface charge. Instead, the more negative zeta potential observed for Nio2 is likely attributable to indirect effects of α-tocopherol on bilayer organization and surface structure, which may facilitate enhanced adsorption of anionic species (e.g., phosphate ions from the buffer) at the vesicle surface [34]. This interpretation is further supported by comparative formulations in which α-tocopherol was replaced with SDS or Phenonip, resulting in less negative zeta potential values (-38 and -30 mV, respectively), indicating that surface charge is governed not solely by the intrinsic charge of individual components but also by their influence on vesicle architecture and interfacial ion distribution. Consistent with our findings, nanoemulsions formulated by Dudek et al. [35] containing α-tocopherol exhibited a negative zeta potential of approximately -40 mV, contributing to colloidal stability, but it is influenced by other components in the formulation rather than tocopherol itself.

3.2.2 | Morphology

The morphology of the niosome formulations was examined using TEM. Figure 1(b) shows that the niosome formulation consists of spherical, large unilamellar vesicles. The variation in texture within the vesicles likely represents the encapsulated standardized water extract of *E. longifolia*. No aggregation of the vesicles was observed in the image, suggesting good colloidal stability under the conditions tested. The observed vesicle size and shape are consistent with the particle size determined by DLS for Nio2, although slightly smaller due to dehydration during sample preparation. The broader size variation observed in TEM compared with the narrow distribution suggested by the 0.05 PDI value may be attributed to differences in the measurement techniques. TEM visualizes individual particles in the dried state and represents only a small portion of the sample, while DLS measures the hydrodynamic size distribution of particles in suspension. Sample preparation and drying during TEM analysis may also contribute to variations in the apparent particle size.

TABLE 2 | Physicochemical properties of *E. longifolia* niosome formulations ($n = 3$).

Sample	Particle size (nm)		PDI	Zeta potential (mV)	EE (%)	Physical appearance
	Day 0	Day 90				
Nio1	193.57 ± 4.35	290.33 ± 13.21	0.11 ± 0.07*	−38.43 ± 1.40	59.50 ± 0.91	Uniform creamy dispersion, no separation layer
Nio2	221.03 ± 0.99	296.93 ± 8.59**	0.05 ± 0.02	−44.90 ± 0.10	65.93 ± 2.99	Uniform creamy dispersion, no separation layer
Nio3	493.16 ± 8.60	539.13 ± 14.48**	0.13 ± 0.05*	−30.63 ± 0.37	66.90 ± 6.62	Uniform creamy dispersion, no separation layer

*$p < 0.05$ compare between Nio2 and Nio3.
**$p < 0.05$ compare between Nio1 and Nio3.

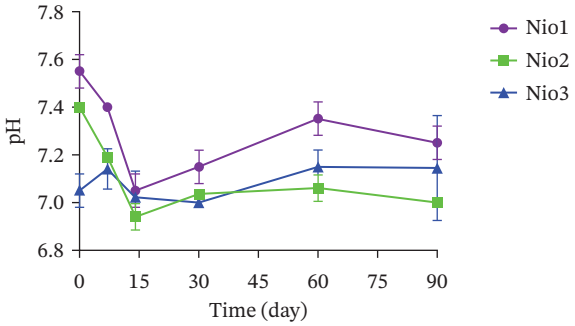

FIGURE 2 | pH values of the niosome formulations within 90 days.

3.2.3 | pH Analysis

The pH value of the hydration medium of niosome formulation plays an important role in the fabrication process and encapsulation efficiency. The pH values recorded for Nio1, Nio2, and Nio3 were 7.55 ± 0.07, 7.35 ± 0.07, and 7.05 ± 0.07, respectively. After 90 days of observation, no significant changes were observed in the pH values of all three formulations ($p > 0.05$), indicating good physicochemical stability during the storage period (Figure 2). Although pH stability alone does not represent the behavior of the formulations under GI condition, nearly neutral pH value of the formulations indicates their compatibility with oral administration. As mentioned by Chang et al. [36], the pH throughout the GI tract varies widely at the stomach to colon within the range of 1–8. Under acidic gastric environments, the stability of the niosomal vesicles may be attributed to their bilayer structure composed of nonionic surfactants (Tween and Span) together with cholesterol. Nonionic surfactants exhibit improved chemical stability, because they are less susceptible to hydrolysis and oxidative degradation under harsh conditions, including acidic environments [37]. Therefore, this allows the vesicular membrane to maintain it structural integrity when exposed to the acidic gastric environment. Furthermore, Span contains long saturated alkyl chains that contribute to increased bilayer rigidity, while Tween provides steric stabilization and improves membrane flexibility. The combined presence of these surfactants helps maintain vesicle integrity and minimize leakage of encapsulated compounds under acidic conditions, which may contribute to the stability of the formulation in the gastric environment [30].

3.2.4 | Stability Analysis

Stability of a formulation can be justified with persistent particle size, no phase separation or precipitation, and no color changes observed from the formulation mixture. After centrifugation at 4000 rpm for 15 min, all three niosome formulations showed good physical stability with no phase separation and color changes (Table 2). Further stability was achieved by storing all three formulations at 24°C for 90 days. No phase separation and color changes are observed for all formulations until up to 90 days. It indicates these formulations remained stable.

The particle size of all formulations showed a gradual increase within 90 days (Figure 3(a)). The particle size of Nio1 started at 193.57 nm on Day 0 and continued to increase to 290.33 nm on Day 90. Formulations Nio2 and Nio3 also showed an increase in particle size from 221.03 nm to 296.93 nm and from 486.16 nm to 539.13 nm (Table 2). The PDI value of Nio1 remained constant from 0.11 on Day 0 until 0.14 on Day 90. The Nio2 formulation exhibited a PDI of approximately 0.04 on Day 0, which increased to 0.24 on Day 90. In contrast, the Nio3 formulation showed a similar pattern of data to Nio1, with an initial PDI value of 0.13 on Day 0, which gradually increased to around 0.18 by Day 90 (Figure 3(b)). These results showed that all niosome formulations remained within the monodisperse to moderately polydisperse range during storage. Statistical analysis using one-way ANOVA confirmed that the changes in both particle size and PDI over time were statistically significant across all formulations, with $p < 0.05$.

The observed differences in stability are closely related to the types of surfactants used in each formulation. Nio1 contained SDS, a surfactant that provides strong electrostatic repulsion between vesicles, which helps to prevent aggregation and contributes to long-term physical stability [27]. Nio2 incorporated α-tocopherol, known for its lipophilic and antioxidant properties, which can enhance bilayer rigidity and protect against oxidative stress, thereby contributing to relatively stable size and PDI values [38]. Overall, these findings indicate acceptable size uniformity and good physical stability of the niosome formulations during the 90-day storage period, demonstrating that appropriate surfactant selection plays a key role in ensuring long-term niosome stability.

3.3 | EE

EE is a crucial parameter for evaluating the performance of niosomal vesicles, as it reflects the system's ability to encapsulate and retain the active compound. Among the tested formulations, Nio3 exhibited the highest EE ($66.90 \pm 6.62\%$), followed closely by Nio2 ($65.93 \pm 2.99\%$) (Table 2). In comparison, Nio1 showed

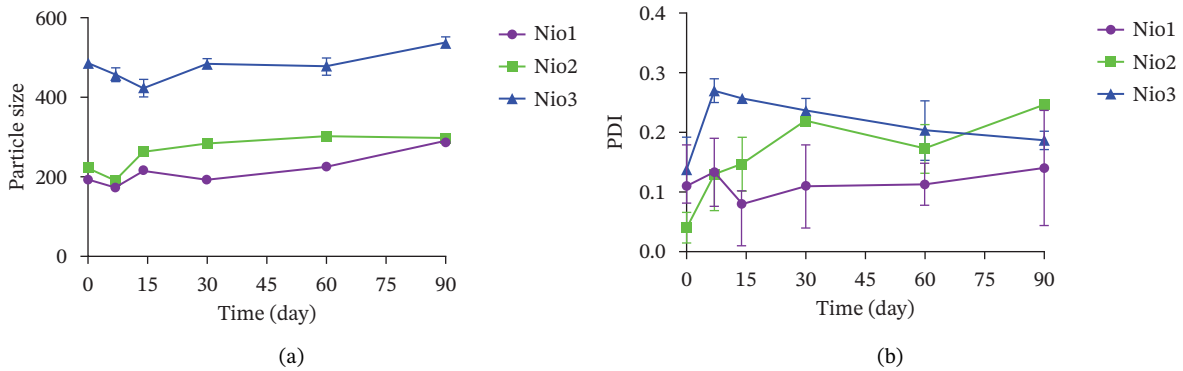

FIGURE 3 | (a) Particle size and (b) PDI values of the niosome formulations over 90 days of storage. Data are presented as mean ± SD ($n = 3$).

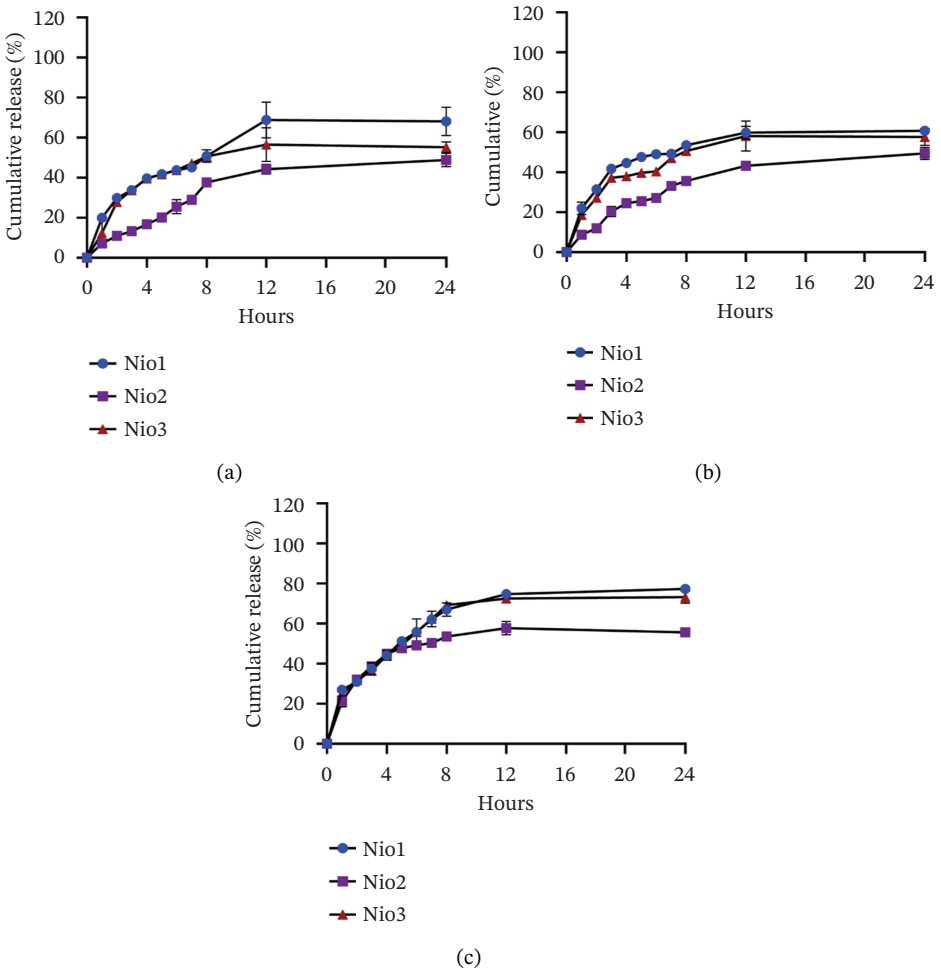

FIGURE 4 | In vitro drug release profile of three niosome formulations at different pH: (a) pH 1.2, (b) pH 6.8, and (c) pH 7.4. Data are presented as mean ± SD ($n = 3$).

the lowest EE% (59.50 ± 0.91%). However, statistical analysis revealed that the differences in EE among the formulations were not statistically significant ($p > 0.05$), indicating that the choice of surfactant did not result in a meaningful variation in drug entrapment under the tested conditions.

3.4 | In Vitro Drug Release Analysis

After 24 h at pH 1.2, Nio1 showed the highest drug release (68.10%), followed by Nio3 (57.68%), while Nio2 exhibited the lowest release (48.80%) (Figure 4(a)). Similarly, at pH 6.8, Nio1 again showed the highest release (60.70%), followed by Nio3 (57.68%) and Nio2 (49.60%) (Figure 4(b)). At pH 7.4, Nio1 maintained the highest release (77.37%), followed by Nio3 (73.25%), while Nio2 remained the lowest (55.66%) (Figure 4(c)). Statistical analysis, however, indicated that the differences in drug release among the three niosome formulations at all tested pH values (1.2, 6.8, and 7.4) were not statistically significant ($p > 0.05$). This may be attributed to the similar EE of the formulations, resulting in comparable amounts of drug available for release. The observed drug release at physiological pH does not necessarily indicate instability of the niosomes system but rather reflects the sustained diffusion of the encapsulated compound through the surfactant–cholesterol bilayer of the vesicles. Niosomes are known to regulate drug permeability through their bilayer membrane, enabling gradual release of entrapped compounds via diffusion, thereby supporting prolonged drug availability under physiological conditions [39]. In addition, the drug release appears to be minimally influenced by environmental pH, leading to parallel release trends across the formulations. Such pH-independent drug delivery systems ensure consistent and reliable drug release under varying pH conditions, helping maintain uniform delivery throughout the GI tract especially beneficial for drugs sensitive to stomach acidity or intestinal alkalinity [40]. Similar controlled release behavior of niosomal formulations at physiological pH has been demonstrated in experimental studies. Study by Rezaei et al. [41] reported sustained drug release from niosomes at pH 7.4 while maintaining vesicle stability, with faster drug release occurring only under acidic conditions. Another study by Barani et al. [42] observed that paclitaxel-loaded niosomes exhibited a prolonged diffusion-controlled release profile at physiological pH compared to the rapid release of the free drug. Therefore, the cumulative release observed remains retained within the vesicles, supporting the controlled release characteristic of the formulation and sufficiently stable at the physiological pH.

The correlation coefficients (R^2) of various kinetic models for eurycomanone release from the three different niosome

TABLE 3 | The correlation coefficient (R^2) for different kinetic models of drug release at different pH for three niosome formulations.

Kinetic model	Correlation coefficient (R^2)								
	pH 1.2			pH 6.8			pH 7.4		
	Nio1	Nio2	Nio3	Nio1	Nio2	Nio3	Nio1	Nio2	Nio3
Zero-order	0.8483	0.9789	0.8904	0.8456	0.9283	0.807	0.8974	0.8654	0.906
First-order	0.9014	0.9817	0.9271	0.901	0.942	0.8463	0.9573	0.9212	0.9626
Higuchi	0.9872	0.9504	0.9691	0.982	0.9625	0.9626	0.989	0.9896	0.9944
Hixson–Crowell	0.8846	0.9812	0.9155	0.8838	0.9376	0.8338	0.9411	0.904	0.9474
Korsmeyer–Peppas	0.8348	0.9054	0.9243	0.8447	0.9254	0.8213	0.8235	0.8596	0.8442

TABLE 4 | IC_{50} values for all samples on three different cell lines.

Sample	IC_{50} (μg/mL)		
	Vero	THP-1	RAW 264.7
Nio1	4.99	4.81	21.32
Nio2	19.90**	23.87**	22.78
Nio3	5.59	5.64	18.64
Standardized water extract of *E. longifolia*	> 62.5**	> 62.5**	> 62.5

**$p < 0.05$ compared with standardized water extract.

formulations at pH 1.2, 6.8, and 7.4 are presented in Table 3. At pH 1.2, all formulations followed the Higuchi model, indicating a diffusion-controlled release mechanism, with Nio1 exhibiting the highest R^2 value (0.9872). Similarly, at pH 6.8, the Higuchi model remained the best fit for all formulations, with Nio1 again showing the highest R^2 value (0.982). At pH 7.4, the Higuchi model continued to dominate, confirming a diffusion-driven release pattern, with Nio3 achieving the highest R^2 value (0.9944). The model with the R^2 value closest to 1 was considered the best-fitting release model for each formulation.

3.5 | Cytotoxicity Analysis of Niosome Formulations

To evaluate the toxicity effects of the niosome formulations encapsulating *E. longifolia* standardized water extract, the formulations were exposed to Vero, THP-1, and RAW 264.7 cell lines at an initial concentration of 62.5 μg/mL, followed by serial dilution. As shown in Table 4, Nio2 exhibited the highest IC_{50} value compared to Nio1 and Nio3. Specifically, the IC_{50} values for Nio2 in the Vero, RAW 264.7, and THP-1 cell lines were 19.90, 22.78, and 23.87 μg/mL, respectively. This indicates that Nio2 required a higher concentration than the other formulations to induce 50% cell death. A higher IC_{50} value suggests a broader range of concentrations can be used before reaching 50% cell death, thereby reducing overall toxicity. Consequently, Nio2 exhibited lower toxicity compared to the other formulations.

Previous studies by Nematollahi et al. [43] have suggested that cholesterol components in niosome formulations can enhance safety by reducing cytotoxicity. Additionally, the standardized *E. longifolia* root water extract showed an $IC_{50} > 62.5$ μg/mL when tested on the three cell lines, indicating that the extract itself was less cytotoxic than the niosome formulations. Statistical analysis revealed that the IC_{50} values of Nio2 were significantly different from those of the standardized *E. longifolia* extract in the Vero and THP-1 cell lines.

Although the standardized *E. longifolia* root water extract exhibited lower cytotoxicity in vitro, the primary objective of niosomal encapsulation in this study was not to reduce the intrinsic cytotoxicity of the extract, but to enable controlled cellular exposure and stabilized delivery of its bioactive constituents. The relatively higher cytotoxicity observed for the niosomal formulations may reflect enhanced interaction and uptake of the encapsulated extract at the cellular level, a phenomenon commonly reported for vesicular delivery systems. This finding seems to contradict the general assumption that niosomes reduce cytotoxicity; however, it may be explained by the penetration of

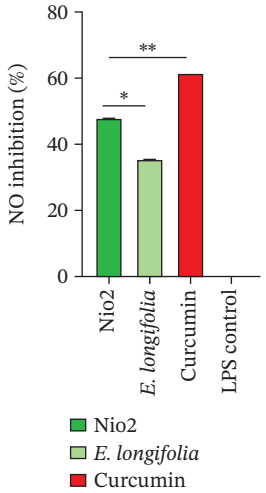

FIGURE 5 | Percentage NO inhibition in LPS-stimulated RAW 264.7 macrophages following treatment with Nio2, *E. longifolia* extract (12.5 μg/mL), and curcumin (positive control). The LPS control group represents cells treated with LPS alone and is expressed as percentage NO inhibition for comparison. **$p < 0.05$ compared to the *E. longifolia*. *$p < 0.05$ compared to the curcumin.

mitochondrial enzyme activity–related proteins on the surface of the niosomes, leading to enzyme denaturation and potentially altering the cytotoxicity results [44]. Interestingly, our findings align with those of Sangkana et al. [45], who reported an IC_{50} of 32.25 μg/mL for their niosome formulation.

Importantly, the Nio2 formulation provided a sufficient safety margin that allowed subsequent biological assays to be conducted at concentrations well below its IC_{50} value, ensuring biological activity while minimizing cytotoxic effects. Therefore, the concentration of Nio2 used in subsequent assays, such as NO release and phagocytic activity, was kept below 23.87 μg/mL to minimize cytotoxic effects.

3.6 | Anti-Inflammatory Activity (NO Inhibition)

The anti-inflammatory activity of the Nio2 formulation and *E. longifolia* extract was assessed using LPS-induced RAW 264.7 macrophage cells, with NO production serving as a key inflammatory biomarker. Excessive NO release is commonly associated with inflammatory responses, and suppression of NO production is widely accepted as an indicator of anti-inflammatory potential. In this study, both Nio2 and *E. longifolia* extract significantly suppressed NO production, with inhibition rates of 47.86% and 35.33%, respectively (Figure 5). These values are notably comparable to that of curcumin (61.36%), a known anti-inflammatory compound used as a positive control. Conversely, the LPS control group, which received no anti-inflammatory treatment, exhibited negligible NO inhibition, reflecting a pronounced inflammatory response. Statistical analysis using one-way ANOVA revealed that the differences in NO inhibition among the treated groups were statistically significant ($p < 0.05$), confirming the efficacy of the treatments.

The comparable NO inhibitory activity observed between Nio2 and the *E. longifolia* extract indicates that encapsulation within a niosome carrier preserves the anti-inflammatory activity of the extract. Although the enhancement in NO inhibition following

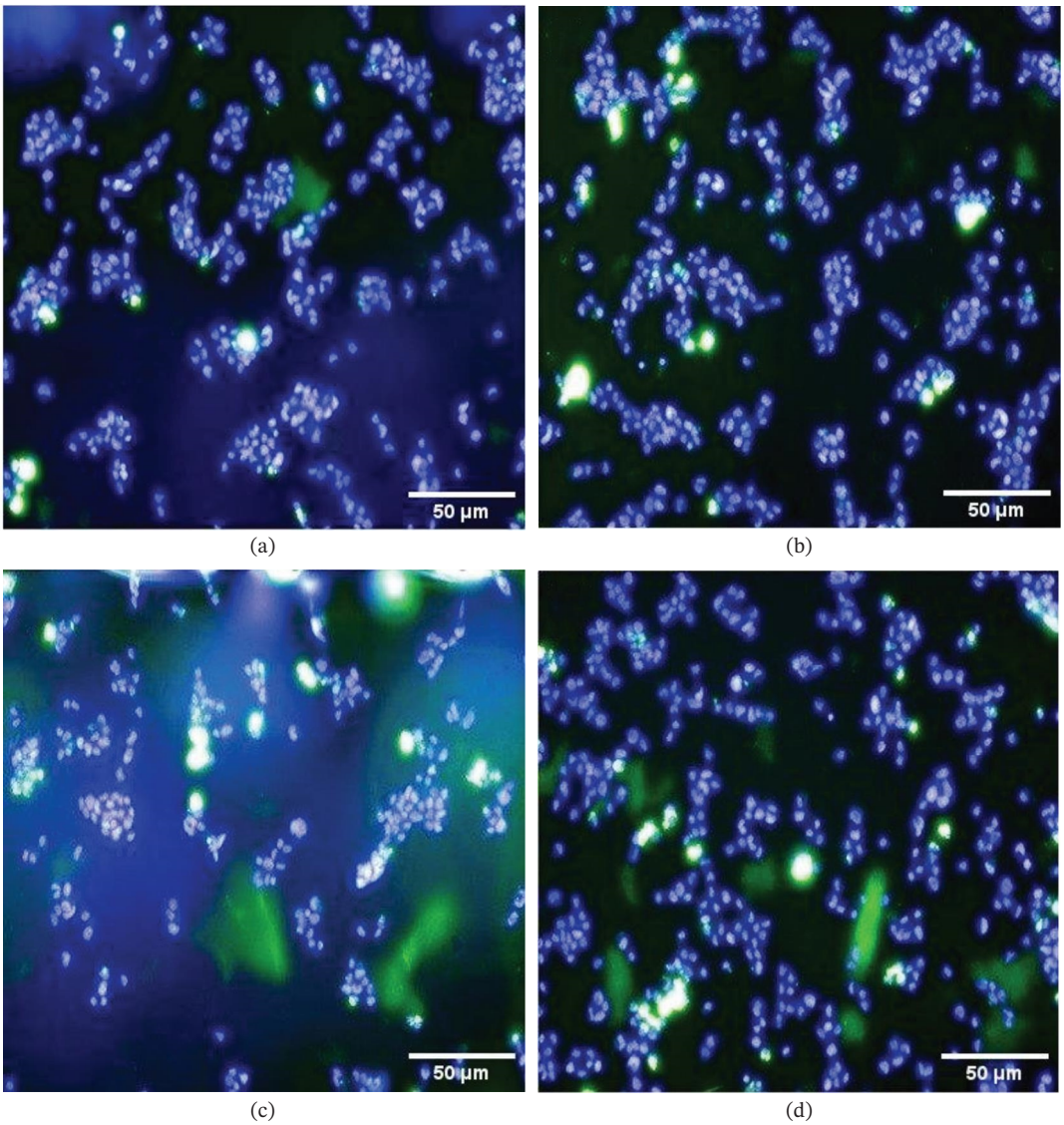

FIGURE 6 | Fluorescence microscopy image of THP-1 cell after treatment with different samples. (a) No treatment, (b) Nio2, (c) *E. longifolia* extract, and (d) curcumin. The cell nuclei are stained with DAPI (4′,6-diamidino-2-phenylindole) and appear bright blue, whereas the Latex Beads–Rabbit IgG–FITC complex appears as green fluorescence.

niosomal encapsulation was modest, this outcome demonstrates that the formulation process did not compromise biological efficacy. Importantly, the intended advantage of the niosomal delivery system in this context is not to markedly amplify short-term in vitro anti-inflammatory potency, but to provide a stabilized delivery platform that enables controlled release and regulated cellular exposure of the bioactive constituents. This finding aligns with a previous study reporting that niosome systems may preserve the anti-inflammatory effects of bioactive compounds in the extract [30].

In agreement with this, Chaingam et al. [10] demonstrated that the NO inhibitory effect of *E. longifolia* extract increases proportionally with dose, likely due to the presence of bioactive compounds such as quassinoids and canthin-6-one alkaloids. Similarly, Zhang et al. [31] reported that these alkaloids effectively inhibit NO production by suppressing pro-inflammatory mediators. Therefore, the ability of the Nio2 formulation to maintain NO inhibitory activity at concentrations below its IC_{50} highlights the role of niosomes as a delivery strategy that balances biological efficacy with controlled exposure, rather than as a direct enhancer of intrinsic bioactivity. Collectively, the results of this study suggest that the Nio2 formulation retains the anti-inflammatory properties of the native extract and holds promise as a post-treatment strategy for inflammatory-related conditions.

3.7 | Phagocytic Activity

The activity of phagocytic of the human macrophage is important to the immune response to protect against pathogens. The effect of niosome formulation on the phagocytic ability of THP-1 cells toward *E. coli* was evaluated. Figure 6 shows the fluorescence image of the cell obtained using a cell content imaging system. The bright blue color represents the nucleus of the cell which is stained by DAPI, while the bright greenish color represents Latex Beads–Rabbit IgG–FITC complex. Thus, this bright greenish color determined the phagocytic activity of THP-1 cells when treated with niosome-encapsulated *E. longifolia* extract. When the cells were treated with Nio2 (Figure 6(b)), the results showed that a higher intensity of greenish color was observed compared to the untreated sample (Figure 6(a)). A similar pattern of greenish color intensity was present when the cells were treated with *E. longifolia* extract (Figure 6(c)) and curcumin (Figure 6(d)). The increases in the phagocytic activity of THP-1 were attributed to macrophage activation after exposure to Nio2, *E. longifolia* extract, and curcumin with the percentage of phagocytic activity values of 4.08%, 4.38%, and 4.47%, respectively. In contrast, the untreated sample showed less phagocytic activity with a value of 2.77% (Figure 7). Statistical analysis demonstrated that the difference between Nio2 and the untreated group was statistically significant ($p < 0.05$).

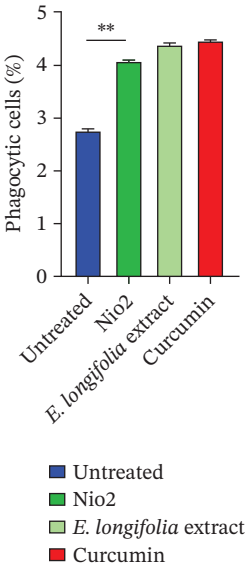

FIGURE 7 | Percentage of phagocytic THP-1 cell after treatment with different samples. $^{**}p < 0.05$ compared to the untreated group.

The comparable phagocytic activity observed between the Nio2 formulation and the *E. longifolia* extract indicates that niosomal encapsulation preserves the immunomodulatory function of the bioactive constituents without impairing macrophage activity. Importantly, the absence of exaggerated or suppressed phagocytic responses following niosomal delivery suggests that the formulation does not induce adverse immune overstimulation, supporting its suitability as a controlled delivery system. These findings are consistent with previous reports indicating that *E. longifolia* extract enhances immunomodulatory activity by promoting the phagocytic ability of RAW 264.7 cells toward *E. coli* [18].

4 | Conclusion

This study successfully developed a stable niosome formulation containing a standardized water extract of *Eurycoma longifolia*. The optimized formulation demonstrated desirable physicochemical properties, good storage stability, high encapsulation efficiency, and controlled, pH-independent release behavior. Biological evaluation showed that the niosomal formulation preserved the immunomodulatory and anti-inflammatory activities of the extract, as demonstrated by NO inhibition and enhanced phagocytic activity in macrophage cell models.

Notably, the observed immunomodulatory and anti-inflammatory effects were comparable to those of the *E. longifolia* extract, indicating that niosome formulation does not compromise the bioactivity of the phytochemical constituents in the *E longifolia* extract. Rather, these findings support the role of niosome as a biocompatible delivery platform capable of maintaining biological efficacy while offering improved formulation stability and controlled cellular exposure. These properties are particularly relevant for overcoming the reported low bioavailability of *E. longifolia* bioactive constituents. Therefore, the developed niosomal formulation represents a promising delivery strategy that warrants further in vivo investigation to confirm its potential to enhance therapeutic performance.

Author Contributions

Muhammad Nor Farhan Saat: writing–original draft, writing–review and editing, project administration, investigation, data curation, validation, and visualization. Norazlinaliza Salim: writing–review and editing, project administration, supervision, data curation, validation, and conceptualization. Wan Abdul Hakim Wan Lokman: data curation and conceptualization. Nabilah Md Razak: data curation and conceptualization. Mohd Ridzuan Mohd Abd Razak: writing–review and editing, supervision, validation, and conceptualization. Mohd Basyaruddin Abdul

Rahman: supervision and conceptualization. Murizal Zainol: conceptualization and resources. Azren Aida Asmawi: methodology and conceptualization.

Acknowledgments

The authors thank the Director General of Health Malaysia for the permission to publish this paper. The study was supported by the Kementerian Kesihatan Malaysia (NMRR-21-668-59501). The scholarship for Muhammad Nor Farhan Saat from the National Institute of Health, Kementerian Kesihatan Malaysia is greatly acknowledged.

Funding

This study was supported by Kementerian Kesihatan Malaysia, NMRR-21-668-59501.

Conflicts of Interest

The authors declare no conflicts of interest.

Data Availability Statement

The data that support the findings of this study are available in the supporting information of this article.

References

1. K. R. Rai, P. Shrestha, B. Yang, et al., "Acute Infection of Viral Pathogens and Their Innate Immune Escape," *Review* 12 (2021): 672026, https://doi.org/10.3389/fmicb.2021.672026.

2. World Health Organisation, "Dengue and Severe Dengue," https://www.who.int/news-room/fact-sheets/detail/dengue-and-severe-dengue.

3. N. H. Md Iderus, S. S. L. Singh, S. M. Ghazali, et al., "The Effects of the COVID-19 Pandemic on Dengue Cases in Malaysia," *Frontiers in Public Health* 11 (2023): 1213514, https://doi.org/10.3389/fpubh.2023.1213514.

4. A. R. K. Patro, S. Mohanty, B. K. Prusty, et al., "Cytokine Signature Associated With Disease Severity in Dengue," *Viruses* 11, no. 1 (2019): 34, https://doi.org/10.3390/v11010034.

5. P. Bhatt, S. P. Sabeena, M. Varma, and G. Arunkumar, "Current Understanding of the Pathogenesis of Dengue Virus Infection," *Current Microbiology* 78, no. 1 (2021): 17–32, https://doi.org/10.1007/s00284-020-02284-w.

6. A. Segaran, L. S. Chua, and N. I. J. L. C. M. Mohd Ismail, "A Narrative Review on Pharmacological Significance of *Eurycoma longifolia* Jack Roots," *Longhua Chinese Medicine* 4 (2021): 2021, https://doi.org/10.21037/lcm-21-32.

7. S. U. Rehman, K. Choe, and H. H. Yoo, "Review on a Traditional Herbal Medicine, *Eurycoma longifolia* Jack (Tongkat Ali): Its Traditional Uses, Chemistry, Evidence-Based Pharmacology and Toxicology," *Molecules* 21, no. 3 (2016): 331, https://doi.org/10.3390/molecules21030331.

8. M. A. Farag, A. O. Ajayi, M. Taleb, K. Wang, and I. M. Ayoub, "A Multifaceted Review of *Eurycoma longifolia* Nutraceutical Bioactives: Production, Extraction, and Analysis in Drugs and Biofluids," *ACS Omega* 8, no. 2 (2023): 1838–1850, https://doi.org/10.1021/acsomega.2c06340.

9. B. Mutschlechner, S. Schwaiger, T. V. A. Tran, and H. Stuppner, "Development of a Selective HPLC-DAD/ELSD Method for the Qualitative and Quantitative Assessment of Commercially Available *Eurycoma longifolia* Products and Plant Extracts," *Fitoterapia* 124 (2018): 188–192, https://doi.org/10.1016/j.fitote.2017.11.015.

10. J. Chaingam, R. Choonong, T. Juengwatanatrakul, T. Kanchanapoom, W. Putalun, and G. Yusakul, "Evaluation of Anti-inflammatory Properties of *Eurycoma longifolia* Jack and *Eurycoma harmandiana* Pierre In Vitro Cultures and Their Constituents," *Food and Agricultural Immunology* 33, no. 1 (2022): 530–545, https://doi.org/10.1080/09540105.2022.2100324.

11. N. Ahmad, D. S. Samiulla, B. P. Teh, et al., "Bioavailability of Eurycomanone in Its Pure Form and in a Standardised *Eurycoma longifolia* Water Extract," *Pharmaceutics* 10, no. 3 (2018): 90, https://doi.org/10.3390/pharmaceutics10030090.

12. S.-H. Lin, Y.-S. Zhao, D.-X. Zhou, F.-C. Zhou, and F. Xu, "Coronavirus Disease 2019 (COVID-19): Cytokine Storms, hyper-Inflammatory Phenotypes, and Acute Respiratory Distress Syndrome," *Genes & Diseases* 7, no. 4 (2020): 520–527, https://doi.org/10.1016/j.gendis.2020.06.009.

13. J.-L. Huo, W.-J. Fu, Z.-H. Liu, N. Lu, X.-Q. Jia, and Z.-S. Liu, "Research Advance of Natural Products in Tumor Immunotherapy," *Review* 13 (2022): 972345, https://doi.org/10.3389/fimmu.2022.972345.

14. K. Radovanović, N. Gavarić, and M. Aćimović, "Anti-Inflammatory Properties of Plants From Serbian Traditional Medicine," *Life* 13, no. 4 (2023): 874, https://www.mdpi.com/2075-1729/13/4/874, https://doi.org/10.3390/life13040874.

15. C. Sitthisak, M. Nisoa, W. Chunglok, et al., "Efficient Extraction of Quassinoids and Alkaloids From *Eurycoma longifolia* Jack Roots Using Natural Deep Eutectic Solvents and Microwave-Assisted Extraction," *Microchemical Journal* 196 (2024): 109676, https://doi.org/10.1016/j.microc.2023.109676.

16. D. T. T. Hien, T. P. Long, T. P. Thao, et al., "Anti-Inflammatory Effects of Alkaloid Enriched Extract From Roots of *Eurycoma longifolia* Jack," *Asian Pacific Journal of Tropical Biomedicine* 9, no. 1 (2019): https://journals.lww.com/aptb/fulltext/2019/09010/anti_inflammatory_effects_of_alkaloid_enriched.3.aspx.

17. J. Ruan, Z. Li, Y. Zhang, et al., "Bioactive Constituents From the Roots of *Eurycoma longifolia*," *Molecules* 24, no. 17 (2019): 3157, https://doi.org/10.3390/molecules24173157.

18. P. He, Z. Dong, Q. Wang, Q.-P. Zhan, M.-M. Zhang, and H. Wu, "Structural Characterization and Immunomodulatory Activity of a Polysaccharide From *Eurycoma longifolia*," *Journal of Natural Products* 82, no. 2 (2019): 169–176, https://doi.org/10.1021/acs.jnatprod.8b00238.

19. L. Huang, S. Luo, S. Tong, Z. Lv, and J. Wu, "The Development of Nanocarriers for Natural Products," *Wiley Interdisciplinary Reviews. Nanomedicine and Nanobiotechnology* 16, no. 3 (2024): e1967, https://doi.org/10.1002/wnan.1967.

20. M. P. Izhar, A. Hafeez, P. Kushwaha, and Simrah, "Drug Delivery Through Niosomes: A Comprehensive Review With Therapeutic Applications," *Journal of Cluster Science* 34, no. 5 (2023): 2257–2273, https://doi.org/10.1007/s10876-023-02423-w.

21. D. B. Momekova, V. E. Gugleva, and P. D. Petrov, "Nanoarchitectonics of Multifunctional Niosomes for Advanced Drug Delivery," *ACS Omega* 6, no. 49 (2021): 33265–33273, https://doi.org/10.1021/acsomega.1c05083.

22. A. Moammeri, M. M. Chegeni, H. Sahrayi, et al., "Current Advances in Niosomes Applications for Drug Delivery and Cancer Treatment," *Materials Today Bio* 23 (2023): 100837, https://doi.org/10.1016/j.mtbio.2023.100837.

23. S. Liga, C. Paul, E.-A. Moacă, and F. Péter, "Niosomes: Composition, Formulation Techniques, and Recent Progress as Delivery Systems in Cancer Therapy," *Pharmaceutics* 16, no. 2 (2024): 223, https://www.mdpi.com/1999-4923/16/2/223, https://doi.org/10.3390/pharmaceutics16020223.

24. N. Shah, R. Prajapati, D. Gohil, P. Sadhu, and S. Patel, "Niosomes: a Promising Novel Nano Carrier for Drug Delivery," *Journal of Pharmaceutical Research International* 33, no. 48B (2021): 53–66, https://doi.org/10.9734/jpri/2021/v33i48B33260.

25. V. Talebi, B. Ghanbarzadeh, H. Hamishehkar, A. Pezeshki, and A. Ostadrahimi, "Effects of Different Stabilizers on Colloidal Properties and Encapsulation Efficiency of Vitamin D3 Loaded Nano-Niosomes," *Journal of Drug Delivery Science and Technology* 61 (2021): 101284, https://doi.org/10.1016/j.jddst.2019.101284.

26. P. Pooprommin, C. Manaspon, A. Dwivedi, et al., "Alginate/Pectin Dressing With Niosomal Mangosteen Extract for Enhanced Wound

Healing: Evaluating Skin Irritation by Structure-Activity Relationship," *Heliyon* 8, no. 12 (2022): e12032, https://doi.org/10.1016/j.heliyon.2022.e12032.

27. N. I. Mohamad Saimi, N. Salim, N. Ahmad, E. Abdulmalek, and M. B. Abdul Rahman, "Aerosolized Niosome Formulation Containing Gemcitabine and Cisplatin for Lung Cancer Treatment: Optimization, Characterization and In Vitro Evaluation," *Pharmaceutics* 13, no. 1 (2021): 59, https://doi.org/10.3390/pharmaceutics13010059.

28. Y. Wang, C. Pi, X. Feng, Y. Hou, L. Zhao, and Y. Wei, "The Influence of Nanoparticle Properties on Oral Bioavailability of Drugs," *International Journal of Nanomedicine* 15 (2020): 6295–6310, https://doi.org/10.2147/ijn.S257269.

29. P. L. Yeo, C. L. Lim, S. M. Chye, A. P. K. Ling, and R. Y. Koh, "Niosomes: A Review of Their Structure, Properties, Methods of Preparation, and Medical Applications," *Asian Biomedicine* 11, no. 4 (2017): 301–314, https://doi.org/10.1515/abm-2018-0002.

30. M. S. Fadaei, M. R. Fadaei, A. E. Kheirieh, et al., "Niosome as a Promising Tool for Increasing the Effectiveness of Anti-Inflammatory Compounds," *EXCLI Journal* 23 (2024): 212–263, https://doi.org/10.17179/excli2023-6868.

31. Y. Zhang, Q. Jing, H. Hu, et al., "Sodium Dodecyl Sulfate Improved Stability and Transdermal Delivery of Salidroside-Encapsulated Niosomes via Effects on Zeta Potential," *International Journal of Pharmaceutics* 580 (2020): 119183, https://doi.org/10.1016/j.ijpharm.2020.119183.

32. S. Karmakar, *Particle Size Distribution and Zeta Potential Based on Dynamic Light Scattering: Techniques to Characterize Stability and Surface Charge Distribution of Charged Colloids (Recent Trends in Materials Physics and Chemistry)* (Studium Press (India)Pvt Ltd, 2019), 117–159.

33. S. J. J. o. c. r. Bhattacharjee, "DLS and Zeta Potential–What They are and What They are Not?" *Journal of Controlled Release* 235 (2016): 337–351, https://doi.org/10.1016/j.jconrel.2016.06.017.

34. G. Duché and J. M. Sanderson, "The Chemical Reactivity of Membrane Lipids," *Chemical Reviews* 124, no. 6 (2024): 3284–3330, https://doi.org/10.1021/acs.chemrev.3c00608.

35. A. Dudek, M. Spiegel, D. Benkowska-Biernacka, M. Domańska, and H. Pruchnik, "Impact of α-Tocopherol Derivatives on the Structural and Functional Properties of Model Lipid Nanocarriers: A Biophysical Modeling Study," *Chemistry and Physics of Lipids* 272 (2025): 105539, https://doi.org/10.1016/j.chemphyslip.2025.105539.

36. H. H. R. Chang, K. Chen, J. A. Lugtu-Pe, et al., "Design and Optimization of a Nanoparticulate Pore Former as a Multifunctional Coating Excipient for," *pH Transition-Independent Controlled Release of Weakly Basic Drugs for Oral Drug Delivery* 15, no. 2 (2023): 547, https://www.mdpi.com/1999-4923/15/2/547, https://doi.org/10.3390/pharmaceutics15020547.

37. X. Ge, M. Wei, S. He, and W. E. Yuan, "Advances of Non-Ionic Surfactant Vesicles (Niosomes) and Their Application in Drug Delivery," *Pharmaceutics* 11, no. 2 (2019): 55, https://doi.org/10.3390/pharmaceutics11020055.

38. D. K. Hincha, "Effects of α-Tocopherol (Vitamin E) on the Stability and Lipid Dynamics of Model Membranes Mimicking the Lipid Composition of Plant Chloroplast Membranes," *FEBS Letters* 582, no. 25 (2008): 3687–3692, https://doi.org/10.1016/j.febslet.2008.10.002.

39. A. Ababei-Bobu, B. Profire, A. T. Iacob, O. M. Chirliu, F. G. Lupaşcu, and L. Profire, "Niosomes as Vesicular Carriers: From Formulation Strategies to Stimuli-Responsive Innovative Modulations for Targeted Drug Delivery," *Pharmaceutics* 17, no. 11 (2025): 1473, https://doi.org/10.3390/pharmaceutics17111473.

40. S. Adepu and S. Ramakrishna, "Controlled Drug Delivery Systems: Current Status and Future Directions," *Molecules* 26, no. 19 (2021): 5905, https://doi.org/10.3390/molecules26195905.

41. T. Rezaei, M. Rezaei, S. Karimifard, et al., "Folic Acid-Decorated pH-Responsive Nanoniosomes with Enhanced Endocytosis for Breast Cancer Therapy: In Vitro Studies," *Frontiers in Pharmacology* 13 (2022): 851242, https://doi.org/10.3389/fphar.2022.851242.

42. M. Barani, M. R. Hajinezhad, S. Sargazi, et al., "In Vitro and In Vivo Anticancer Effect of pH-Responsive Paclitaxel-Loaded Niosomes," *Journal of Materials Science: Materials in Medicine* 32, no. 12 (2021): 147, https://doi.org/10.1007/s10856-021-06623-6.

43. M. H. Nematollahi, A. Pardakhty, M. Torkzadeh-Mahanai, M. Mehrabani, and G. Asadikaram, "Changes in Physical and Chemical Properties of Niosome Membrane Induced by Cholesterol: A Promising Approach for Niosome Bilayer Intervention," *RSC Advances* 7, no. 78 (2017): 49463–49472, https://doi.org/10.1039/C7RA07834J.

44. M. Awashra and P. Młynarz, "The Toxicity of Nanoparticles and Their Interaction With Cells: An In Vitro Metabolomic Perspective," *Nanoscale Advances* 5, no. 10 (2023): 2674–2723, https://doi.org/10.1039/d2na00534d.

45. S. Sangkana, K. Eawsakul, T. Ongtanasup, et al., "Preparation and Evaluation of a Niosomal Delivery System Containing *G. mangostana* Extract and Study of Its Anti-Acanthamoeba Activity," *Nanoscale Advances* 6, no. 5 (2024): 1467–1479, https://doi.org/10.1039/D3NA01016C.

Supporting Information

Additional supporting information can be found online in the Supporting Information section. **Supporting Information.** Table S1. Preliminary screening—Composition and characterization of niosome formulations.